DEVELOPMENTAL DYNAMICS 00:00–00, 2017
DOI: 10.1002/DVDY.24531

Cx43 Suppresses *evx1* Expression to Regulate Joint Initiation in the Regenerating Fin

Gabrielle Dardis,[1] Robert Tryon,[2] Quynh Ton,[1] Stephen L. Johnson,[2] and M. Kathryn Iovine[1]*

[1]Department of Biological Sciences, Lehigh University, Bethlehem, Pennsylvania
[2]Genetics Department, Washington University School of Medicine, St. Louis, Missouri

Background: How joints are correctly positioned in the vertebrate skeleton remains poorly understood. From our studies on the regenerating fin, we have evidence that the gap junction protein Cx43 suppresses joint formation by suppressing the expression of the *evx1* transcription factor. Joint morphogenesis proceeds through at least two discrete stages. First, cells that will produce the joint condense in a single row on the bone matrix ("initiation"). Second, these cells separate coincident with articulation of the bone matrix. We propose that Cx43 activity is transiently reduced prior to joint initiation. Results: We first define the timing of joint initiation with respect to regeneration. We next correlate reduced *cx43* expression and increased *evx1* expression with initiation. Through manipulation of *cx43* expression, we demonstrate that Cx43 negatively influences *evx1* expression and joint formation. We further demonstrate that Cx43 activity in the dermal fibroblasts is required to rescue joint formation in the *cx43* mutant, *short fin*^{b123}. Conclusions: We conclude that Cx43 activity in the dermal fibroblasts influences the expression of *evx1*, and therefore the differentiation of the precursor cells that give rise to the joint-forming osteoblasts. *Developmental Dynamics 000:000–000, 2017*. © 2017 Wiley Periodicals, Inc.

Key words: skeletal regeneration; Zebrafish; gap junction; interzone

Submitted 7 March 2017; First Decision 8 May 2017; Accepted 30 May 2017; Published online 0 Month 2017

Introduction

Proper skeletal development and joint placement are necessary for normal vertebrate structure and movement, yet the molecular mechanisms underlying these events are poorly understood. We utilize the Zebrafish regenerating-fin model to provide insights into mechanisms regulating bone growth and joint formation. The fin comprises multiple bony fin rays, each composed of multiple bony segments separated by joints. Following amputation, the fin rapidly restores its size and pattern during regenerative growth, allowing for extended opportunities to study segment length and joint formation. New growth occurs at the distal end, therefore younger tissue is always located distal to older tissue (Brown et al., 2009).

Each fin ray is composed of two hemirays of bone matrix that surround a central mesenchyme. During regeneration, the rapidly dividing cells of the blastema are located medially (and distally), and the differentiating skeletal precursor cells of the osteoblast lineage (i.e., precursors of osteoblasts and joint-forming cells) are located laterally and essentially surround the dividing cells. Clonal analysis of fin growth and regeneration reveals nine lineage classes that contribute to the adult fin (Knopf et al., 2011; Tu and Johnson, 2011). Two of these lineages are responsible for the skeletal elements of the fin. These are the osteoblast lineage, including both bone-forming cells and joint-forming cells, and the dermal fibroblast lineage, which includes the loose mesenchymal cells. The first overt sign that a joint will be produced occurs when joint-forming osteoblasts condense as a single row on the surface of the bone matrix ("initiation"). These cells subsequently mature into two rows of joint-forming cells that surround the newly articulated joint (Sims et al., 2009). Earlier events of joint morphogenesis are poorly understood, including how joint-forming cells are instructed to differentiate and to give rise to a joint in the appropriate location.

Our research suggests that the gap junction protein Cx43 influences how these decisions are made (Sims et al., 2009; Ton and Iovine, 2013b). Hypomorphic mutations in *cx43* are responsible for the *short fin* (*sof*^{b123}) mutant phenotypes, which include short fins, short bony fin ray segments, and reduced cell proliferation (Iovine et al., 2005). Both *cx43* mRNA and Cx43 protein are expressed throughout the medial fin ray mesenchyme (including in dividing cells) and in the adjacent joint-forming cells (Hoptak-Solga et al., 2008; Sims et al., 2009). Our findings reveal that Cx43 function (in one or both of these cellular compartments) is responsible for coordinating skeletal growth with skeletal patterning. An additional mutant, *another long fin* (*alf*^{dty86}, with a mutation in *kcnk5b*) (Perathoner et al., 2014), exhibits increased *cx43* mRNA levels and overlong segments and fins (Sims et al., 2009; van Eeden et al., 1996). However, because segment length

Grant sponsor: NIH; Grant number: R15HD080507; Grant sponsor: NIH; Grant number: R01GM056988.
*Correspondence to: M. Kathryn Iovine, Department of Biological Sciences, 111 Research Drive, Lehigh University, Bethlehem, PA 18015. E-mail: mki3@lehigh.edu

Article is online at: http://onlinelibrary.wiley.com/doi/10.1002/dvdy.24531/abstract
© 2017 Wiley Periodicals, Inc.

is rescued in *alf*^{dty86} regenerating fins following *cx43* knockdown, we have suggested that Cx43 suppresses joint formation. This has led to models whereby the long segment phenotype of *alf*^{dty86} is due to stochastic joint failure, and the short segment phenotype of *sof*^{b123} is due to premature joint formation.

The earliest known gene required for joint formation is the *even-skipped transcription factor 1* (*evx1*) (Schulte et al., 2011). The *evx1* gene is expressed in a single band of cells at the distal end of fin rays as they produce joints (Borday et al., 2001). Regenerating fins in *alf*^{dty86} mutants show stochastic *evx1* expression (consistent with stochastic joint failure), which, remarkably, is rescued by *cx43*-knockdown (Ton and Iovine, 2013b). Thus, we suggest that Cx43 suppresses joint formation in *alf*^{dty86} by suppressing *evx1* expression. In contrast, *sof*^{b123} mutants exhibit *evx1* expression in regenerating fin rays more distally than in wild-type (Ton and Iovine, 2013b), consistent with the hypothesis that joint formation is premature. Together, these findings suggest a model in which the differentiation of joint-forming cells is suppressed by Cx43 function in a way that permits joint-forming cells to differentiate at the appropriate time and place. This model predicts that Cx43 function must be reduced for joint initiation to occur. Here, we provide support for this model by showing that *cx43* expression is negatively correlated with joint initiation, and we demonstrate that manipulation of Cx43 activity influences both the expression of *evx1* and joint formation. Moreover, we demonstrate that Cx43 function in the dermal fibroblast lineage, but not in joint-forming osteoblasts, is required to rescue both regenerate length and segment length in *sof*^{b123} fins. This study provides evidence that Cx43 function suppresses the joint-forming cell fate in a non-autonomous manner.

Results

Cx43 Function is Reduced When Joint Formation is Initiated

In order to monitor Cx43 activity during joint formation, we first identified a time line for joint initiation during regeneration. Our prior studies on joint morphogenesis identified ZNS5-positive cell condensations, similar to the interzone cells of synovial joints, that predict the location of the future joint (Sims et al., 2009). Distally, ZNS5-positive joint cells exhibited an elongated morphology in a single row of cells during joint "initiation." More proximally,

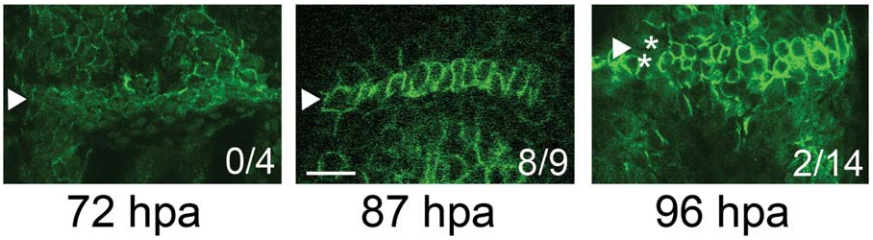

Fig. 1. Establishment of the joint initiation time line. Fins were amputated at the 30% level and permitted to regenerate for 2–5 days before processing for ZNS5 immunofluorescence. Selected time points are shown. Fins at 87 hpa frequently exhibited "initiating" joints in the third fin ray from the dorsal or ventral side. The ratios in each image indicate the frequency of initiating joints at each time point. Arrowheads indicate the organizing joint-forming cells, and the asterisks in 96 hpa identify the separating rows of joint-forming cells. Scale bar = 20 μm.

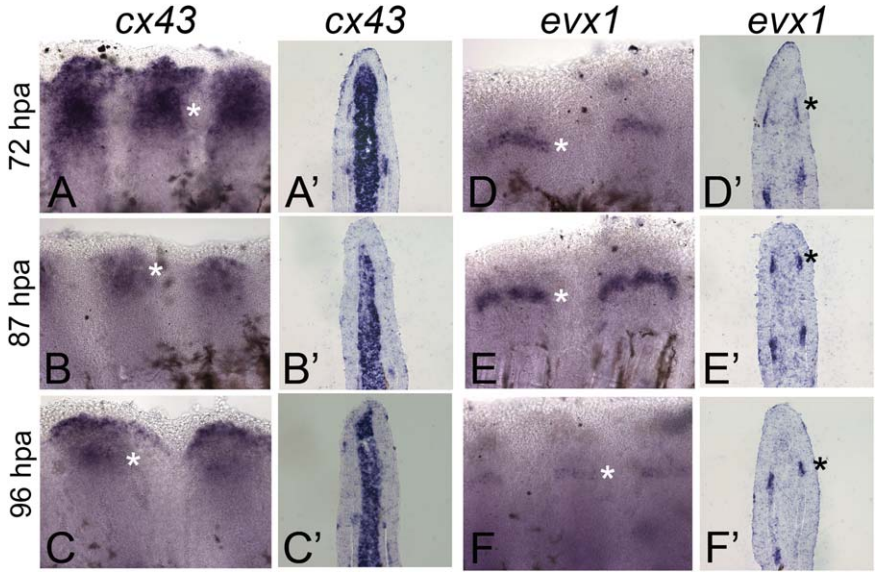

Fig. 2. Expression of *cx43* and *evx1* during the joint initiation time line. Qualitative changes in *cx43* and *evx1* gene expression are shown. Whole-mount ISH for *cx43* is shown at 72 hpf (**A**), 87 hpf (**B**), and 96 hpf (**C**). Cryo-ISH for *cx43* is shown at 72 hpa (**A'**), 87 hpf (**B'**), and 96 hpf (**C'**). Whole-mount ISH for *evx1* is shown at 72 hpf (**D**), 87 hpf (**E**), and 96 hpf (**F**). Cryo-ISH for *evx1* is shown at 72 hpa (**D'**), 87 hpf (**E'**), and 96 hpf (**F'**). Asterisks identify regions of gene expression. Note that *cx43* mRNA is detected medially in the dermal fibroblasts and laterally in a subset of cells in the osteoblast lineage, whereas *evx1* mRNA is restricted to a subset of cells in the osteoblast lineage.

TABLE 1. [a]ΔC_T Values for *cx43* and *evx1* During the Joint Initiation Time Course[a]

Biological replicates	*cx43* 72 hpa	*cx43* 87 hpa	*cx43* 96 hpa	*evx1* 72 hpa	*evx1* 87 hpa	*evx1* 96 hpa
1	3.27	5.41	4.23	9.84	9.28	9.68
2	2.88	4.48	3.39	8.11	3.31	8.19
3	3.16	4.24	3.98	11.37	10.35	12.76

[a]ΔC_T values are determined by subtracting the average *actin* C_T value from the average C_T value for either *cx43* or *evx1*.

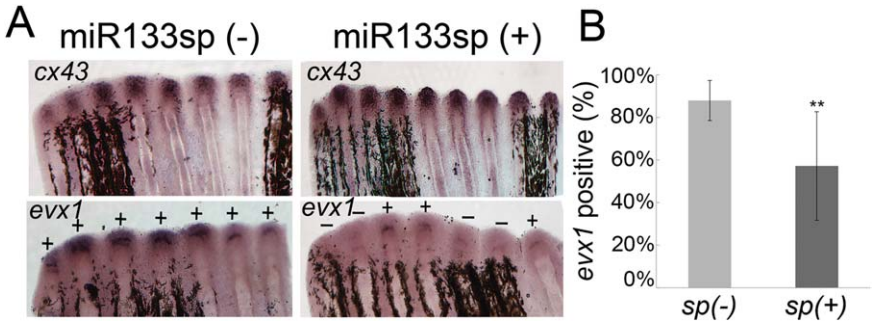

Fig. 3. Increased *cx43* at the time of joint formation reduces the frequency of *evx1*-positive rays. **A**: Whole-mount ISH shows increased *cx43* and decreased *evx1* expression at the time of joint initiation (87 hpa) in the *Tg(hsp70:miR-133sp)*^{pd48} line following a heat pulse at 72 hpa. Transgene-positive fins, sp(+) (n = 9 fins), were compared to nontransgenic sp(-) siblings (n = 7 fins). **B**: The sp(+) transgenic fish showed reduced frequency of *evx1* expression compared to the sp(-) nontransgenic sibling. Both sp(+) and sp(-) fish were similarly treated for heat shock. Statistically significant differences were determined by the Student's *t*-test, where $P < 0.01$ (**). Error bars represent the standard deviation.

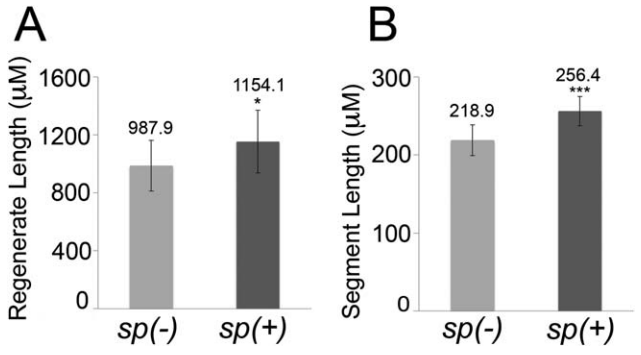

Fig. 4. Increased *cx43* in the *Tg(hsp70:miR-133sp)*^{pd48} line leads to an increase in regenerate length (**A**) and segment length (**B**) in sp(+) (transgene-positive, n = 12) compared to similarly treated sp(-) siblings (n = 10). Both sp(+) and sp(-) fish were similarly treated for heat shock. Statistically significant differences were determined by the Student's *t*-test, where $P < 0.05$ (*) or $P < 0.001$ (***). Error bars represent the standard deviation.

joint-forming cells appeared to separate away from each other and, finally, joint cells were located in two rows of cuboidal cells on either side of the articulation in the bone matrix. These prior studies were completed on a population of fin rays at 5 days post-amputation (dpa). To establish a time line for the initiation phase of joints, we monitored distal ZNS5-positive condensation of elongated cells from a single fin ray (i.e., the third fin ray from either the dorsal-most or ventral-most side of the fin) over time. Since the rate of regeneration is more rapid following proximal amputations (Lee et al., 2005), we amputated fins slightly more distally to increase the amount of time between transitions in joint morphology; amputations were performed at the 30% level vs. the 50% level. During this time course, ZNS5-positive cells were in initiation at about 87 hr post-amputation (hpa) (Fig. 1).

Next, we wished to correlate Cx43 activity during the time line. We followed *cx43* mRNA levels pre-initiation (72 hpa), at initiation (87 hpa), and post-initiation (96 hpa) using both whole-mount in site hybridization (ISH) and cryosection ISH to visualize the qualitative changes in expression levels of *cx43* mRNA. It is important to note that we observed a modest but detectable reduction in *cx43* mRNA levels at 87 hpa (Fig. 2). Because *evx1* is required for joint formation (Schulte et al., 2011), we correlated its expression during the joint formation time line. In contrast to *cx43*, we observed an increase in *evx1* mRNA levels at 87 hpa by both whole-mount ISH and by ISH on cyrosections (Fig. 2). Therefore, we find a negative correlation between *cx43* and joint initiation and a positive correlation between *evx1* and joint formation.

We additionally utilized quantitative RT-PCR (qRT-PCR) to further demonstrate the differences in *cx43* and *evx1* mRNA levels in a more quantitative manner. We compared ΔC_T values between samples of different time points, where ΔC_T represents the normalized cycle when the threshold for detection is reached. Therefore, higher ΔC_T values indicate lower levels of template mRNA, whereas lower ΔC_T values indicate higher levels of template mRNA. Indeed, we found that ΔC_T values were increased for *cx43* at 87 hpa and decreased for *evx1* at 87 hpa in three independent biological replicates (Table 1), consistent with our ISH results. We note that while the three replicates consistently indicate relatively higher *evx1* expression at 87 hpa, the results are somewhat variable. We attribute this finding to the fact that

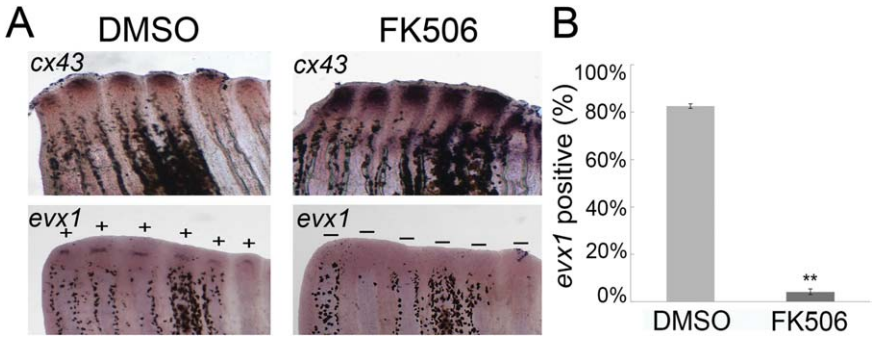

Fig. 5. Inhibition of calcineurin (FK506-treatment) increases *cx43* and reduces the frequency of *evx1*-positive rays. **A**: Whole-mount ISH shows increased *cx43* and decreased *evx1* expression at the time of joint initiation (87 hpa) in FK506-treated fish vs. DMSO (negative control). **B**: FK506-treated fish (n = 3 fins) showed reduced frequency of *evx1*-positive fin rays compared to DMSO-treated fish (n = 4 fins). Statistically significant differences were determined by the Student's *t*-test, where $P < 0.01$ (**). Error bars represent the standard deviation.

relatively few cells express *evx1* specific to the most distal joint within the regenerating tissue. Overall, the qRT-PCR results confirm our findings by ISH and provide evidence that *cx43* mRNA levels are reduced during joint initiation whereas *evx1* mRNA levels are increased.

Increased Cx43 Reduces the Frequency of evx1-positive Rays and Influences Segment Length

Based on the above correlative studies, we predict that the manipulation of Cx43 activity will influence both *evx1* expression and joint initiation. For example, increasing Cx43 function prior to joint initiation should inhibit *evx1* expression and delay joint initiation, leading to joint failure or overlong segments. To overexpress Cx43, we took advantage of a transgenic line created to inhibit *miR-133a*, which targets *cx43* mRNA for degradation (Yin et al., 2012). Inhibition of *miR-133* is accomplished by inserting several *miR-133*-binding sequences upstream of enhanced green fluorescent protein (*egfp*) and downstream of an inducible heat shock promoter, *hsp70*. This line, referred to as the "sponge" line (*Tg[hsp70:miR-133sp]*^{pd48}), sequesters endogenous *miR133a* and therefore increases *cx43* expression (note that *evx1* does not have the predicted *miR-133a*-binding site) (Yin et al., 2012). Indeed, we find that *cx43* levels are increased in *Tg(hsp70:miR-133sp)*^{pd48} at 24 hr following a 1-hr heat pulse (Fig. 3). Moreover, in a prior study, we showed that Cx43 protein levels are increased by 50% in *Tg(hsp70:miR-133sp)*^{pd48} treated with a heat pulse compared to similarly treated nontransgenic siblings (Banerji et al., 2016).

We tested if increased *cx43* influences *evx1* expression at the time of joint initiation. Fins were amputated at the 30% level, followed by a 1-hr heat pulse at 72 hpa (pre-initiation) in *Tg(hsp70:miR-133sp)*^{pd48}. We harvested fins at 87 hpa (initiation) and evaluated *evx1* expression compared to nontransgenic siblings that received the same treatment. Since elevated *cx43* in *alf*^{dty86} fins causes stochastic *evx1* expression (Ton and Iovine, 2013b), we calculated the percentage of rays expressing *evx1* (*evx1*-positive) rather than evaluate expression qualitatively. We compared the percent of *evx1*-positive fin rays across the entire fin between *Tg(hsp70:miR-133sp)*^{pd48} and nontransgenic siblings. As expected, we found a significant decrease in the percentage of *evx1*-positive fin rays in *Tg(hsp70:miR-133sp)*^{pd48} fins, from 87.9% (109/126 fin rays) in the nontransgenic sibling to 57.2% (94/179 fin rays) in the sponge line (Fig. 3).

Following the same timing of amputation and heat treatment, we next measured regenerate length and segment length (i.e., as a proxy for joint formation) by harvesting at 96 hr post–heat shock induction. We found a significant increase in both regenerate length and segment length in the *Tg(hsp70:miR-133sp)*^{pd48} line compared to the nontransgenic siblings (Fig. 4).

To supplement our transgenic manipulation of Cx43 expression levels, we additionally treated wild-type Zebrafish with FK506 (tacrolimus), a calcineurin inhibitor that results in increased fin length and increased *cx43* expression (Kujawski et al., 2014). FK506-treated populations were compared to control populations treated with DMSO. To evaluate changes in *cx43* and *evx1* expression, fish were treated at 72 hpa with FK506 for 15 hr and harvested 87 hpa (initiation). Whole-mount ISH was conducted to visualize expression levels of *cx43* and *evx1* mRNA. We observed an increase in *cx43* expression in regenerating fins from FK506-treated fish, and a reduction in the percentage of *evx1*-positive fin rays from 81.3% (48/59 fin rays) in DMSO-treated to 4.1% (2/49 fin rays) in FK506 treated (Fig. 5). To evaluate regenerate length and segment length, fish were treated with FK506 for 3 consecutive days (starting at 48 hpa and harvesting at 120 hpa). Calcein staining was used to detect bone matrix and joints between segments. We found a significant increase in regenerate length in fish treated with FK506 (Fig. 6). Additionally, while control DMSO-treated fish developed 1–2 joints per fin ray, FK506-treated fish failed to develop any joints during the observed time period, and therefore segment length could not be measured (Fig. 6). These results indicate that increased *cx43* levels decrease the number of fin rays expressing *evx1*, decrease the number of fin rays that produce joints, and cause joint delay/overlong segments. These findings support our model that overexpression of *cx43* causes the failure of both *evx1* expression and of joint initiation.

Decreased Cx43 Activity Leads to Premature evx1 Expression and Reduced Segment Length

Decreasing *cx43* function is predicted to cause premature *evx1* expression and premature joint initiation, leading to short segments. Indeed, in a prior study we found that *sof*^{b123} mutants exhibit these phenotypes (Ton and Iovine, 2013b). In order to study the effects of *cx43* depletion independently, a transgenic line that overexpresses *miR-133* was utilized (i.e., *Tg(hsp70:miR-133a1)*^{pd47}) (Yin et al., 2012). This line reduces *cx43* expression. Indeed, following a 1-hr 37°C heat shock, we find that *cx43* levels are reduced in the *Tg(hsp70:miR-133a1)*^{pd47} (Fig. 7).

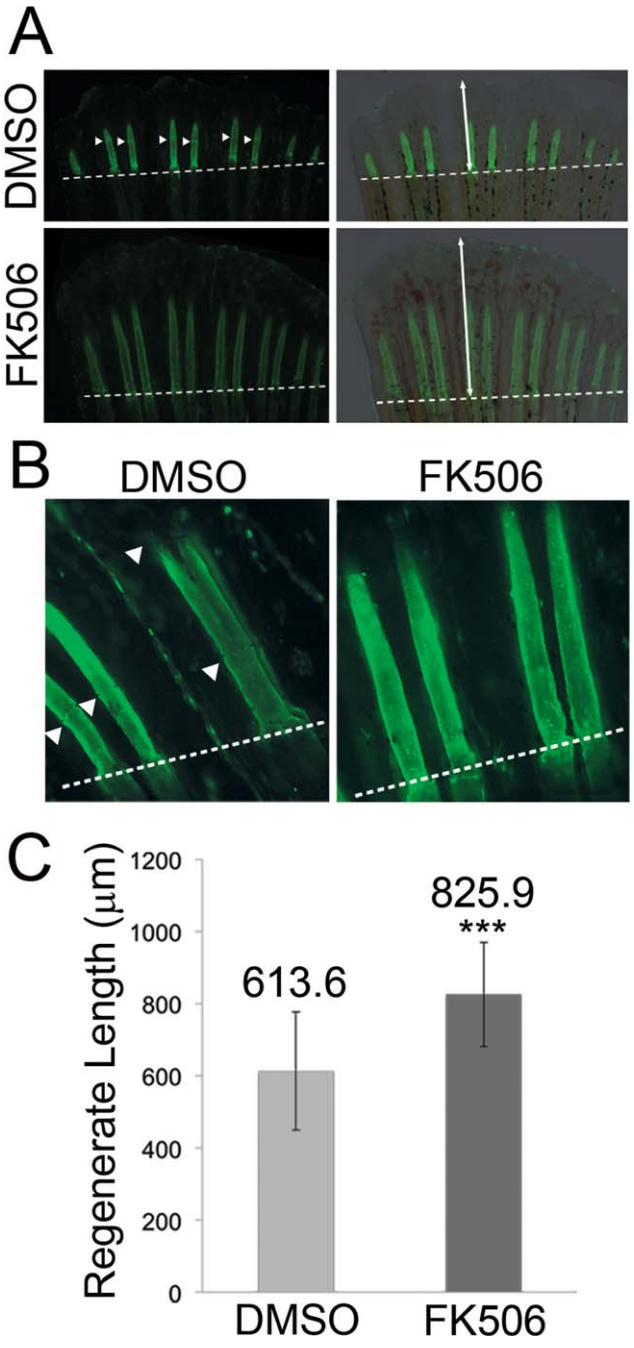

Fig. 6. Inhibition of calcineurin (FK506 treatment) influences joint formation and regenerate length. **A,B**: Calcein staining detects bone matrix and reveals joint failure and increased regenerate length in FK506-treated wild-type fish compared to control DMSO-treated wild-type fish. Panels on the left show fluorescence; panels on the right show fluorescence plus bright-field to better illustrate the end of the regenerating fin (the dotted line indicates the amputation plane). Arrowheads point to joints. Double-headed arrows identify regenerate length. **C**: Regenerate length is significantly increased FK506-treated (n = 18) vs. DMSO-treated (n = 18, negative control) fish. Statistically significant differences were determined by the Student's *t*-test, where $P < 0.001$ (***). Error bars represent the standard deviation.

We tested if decreased Cx43 influences *evx1* expression at the time of joint initiation. Fins were amputated at the 30% level, followed by a 1-hr heat pulse at 72 hpa (pre-initiation) in the *Tg(hsp70:miR-133a1)*^{pd47}. To confirm activation after heat shock, as there is no *egfp* encoded in the *miR-133a* transgene, *miR-133sp* fish with the EGFP indicator were amputated along the same time line and added to heat shock tanks. GFP was observed in the *miR-133sp* indicator fish post–heat shock, indicating that the heat shock was effective. To determine whether decreased *cx43* expression influences *evx1* expression, fins were harvested at 87 hpa and processed for *evx1* ISH. In contrast to the *miR-133a* sponge line, the percentage of *evx1*-positive fin rays increased in *Tg(hsp70:miR-133a1)*^{pd47} regenerating fins, from 51% (87/170 fin rays) in the nontransgenic siblings to 79.5% (132/166 fin rays) in the *miR-133* overexpression line (Fig. 7).

We next measured regenerate length and segment length using calcein staining at 96 hr post–heat shock induction. While regenerate length appears shorter in the *Tg(hsp70:miR-133a1)*^{pd47} line compared to nontransgenic siblings, this difference is not significant. Therefore, transiently reducing *cx43* expression at 72 hr is not sufficient to impact the rate of regeneration over several days. In contrast, we found a significant decrease in segment length in *Tg(hsp70:miR-133a1)*^{pd47} compared to nontransgenic siblings (Fig. 8). These results indicate that decreased *cx43* levels in wild-type lead to premature expression of *evx1*, which in turn leads to premature joint initiation and, therefore, shortened segments. These findings support our model that reduced expression of *cx43* permits premature *evx1* expression and joint initiation.

Cx43 Function in Dermal Fibroblasts is Sufficient for Cx43-dependent Skeletal Growth and Patterning

Because Cx43 is expressed in both the medial dermal fibroblasts and the lateral joint-forming osteoblasts, one possibility is that Cx43 functions autonomously in each population to coordinate skeletal growth (cell proliferation) and patterning (joint formation). Alternatively, Cx43 function in a single cell population could be responsible for both Cx43-dependent phenotypes. We chose to distinguish these possibilities by performing clonal analyses in *sof*^{b123} regenerating fins (as we have done before to demonstrate that expression of *kitlga* in dermal fibroblasts rescues the *kit ligand a* mutant phenotype) (Tryon and Johnson, 2014). The *cx43* coding sequence was inserted into the hsp-PT2 transposon plasmid behind the *hsp70l* promoter and together with the *ef1a-egfp* cassette. The latter element drives ubiquitous expression of GFP and therefore permits detection of clones in the absence of heat shock. This construct, plus transposase, was injected into one-cell *sof*^{b123} embryos. All GFP-positive fish were raised and screened for caudal fin clones in adults. GFP-positive fin clones were assigned to one of the lineage classes based on morphology (as described in Tu and Johnson, 2011). Clones were amputated in the middle of the clone, and regeneration proceeded with a daily heat pulse to induce transient overexpression of the *cx43* transgene. Remarkably, while GFP-positive cells were identified in multiple cell lineages, only GFP-positive clones in the dermal fibroblasts reliably rescued the *sof*^{b123} growth phenotypes (Table 2). The occasional rescue of the *sof*^{b123} phenotypes by epidermal clones is ascribed to these clones masking underlying dermal fibroblast clones. The level of rescue of regenerate length and segment length phenotypes was measured by comparing the ratios of fin ray length or segment length from fin rays within the GFP-positive clone to the contralateral GFP-negative fin rays at the same position (Fig. 9). The rescue of segment length by Cx43 requires that both *evx1* expression and joint formation are delayed in the context of *sof*^{b123} regenerating fins, although only joint formation was evaluated. Although we propose that Cx43

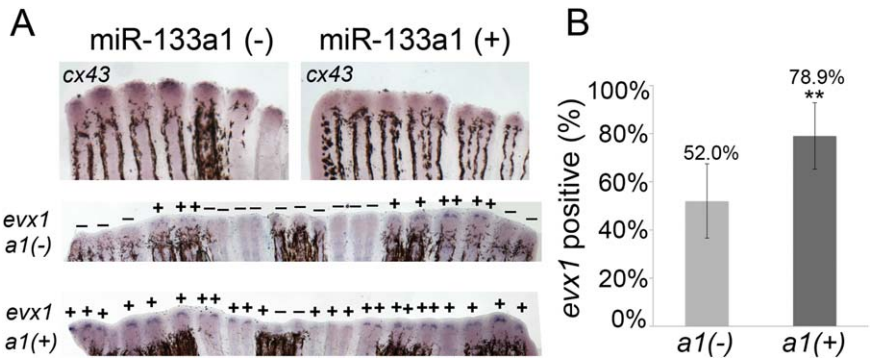

Fig. 7. Reduced *cx43* prior to joint formation increases the frequency of *evx1*-positive rays. **A**: Whole-mount ISH shows decreased *cx43* expression and increased *evx1* expression in the *Tg(hsp70:miR-133a1)*^{pd47} line at the time of joint initiation (87 hpa) in a1(+) (transgene-positive) vs. a1(-) (nontransgenic). Bottom panels in A show *evx1*-positive fin rays across entire fins. **B**: A higher percentage of fin rays in a1(+) transgenic fins showed expression of *evx1* (n = 9 fins) compared to the a1(-) nontransgenic sibling (n = 9 fins). Both sp(+) and sp(-) fish were similarly treated for heat shock. Statistically significant differences were determined by the Student's *t*-test, where $P < 0.01$ (**). Error bars represent the standard deviation.

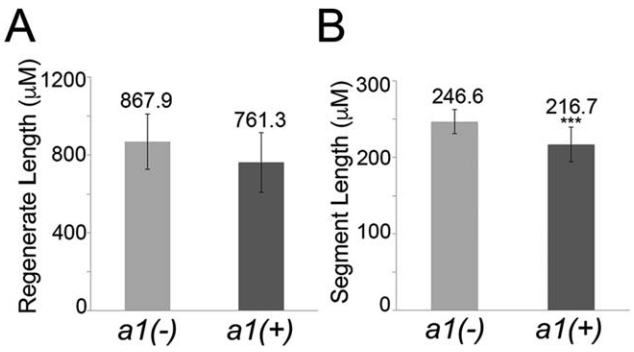

Fig. 8. Decreased *cx43* in the *Tg(hsp70:miR-133a1)*^{pd47} line influences segment length.Regenerate length (**A**) is not significantly decreased, whereas segment length (**B**) is significantly decreased in a1(+) (transgene-positive; n = 16) compared with nontransgenic a1(-) siblings (n = 12). Both a1(+) and a1(-) fish were similarly treated for heat shock. Statistically significant differences were determined by the Student's *t*-test, where $P < 0.001$ (***). Error bars represent the standard deviation.

suppresses *evx1*/joint formation, the transient nature of Cx43 overexpression prevents complete inhibition of joint formation, and rather delays joint formation so that segment length is increased. These data demonstrate that Cx43 activity in dermal fibroblasts both promotes fin ray length (i.e., increased ray length) and suppresses joint formation (i.e., increased segment length), and further suggests that medially located Cx43-positive cells communicate with cells in both the medial and lateral mesenchyme to influence cell proliferation and cell differentiation.

Discussion

How the precise location of joints in the skeleton is determined is poorly understood. In prior studies, we showed that joint formation in fin ray joints "initiates" with the condensation of joint-forming cells (analogous to the interzone in synovial joints) (Pacifici et al., 2006), and that reducing Cx43 levels in *alf*^{dty86} mutants rescues both segment length and *evx1* expression (Sims et al., 2009; Ton and Iovine, 2013b). Here, we connect joint initiation with *cx43* and *evx1* expression by revealing a time line for joint initiation, by negatively correlating changes in *cx43* with joint initiation, by positively correlating changes in *evx1* expression with joint initiation, and by showing that manipulation of Cx43 influences both *evx1* expression and joint initiation. These studies, together with our earlier studies, suggest that a threshold of Cx43 activity determines whether or not *evx1* will be expressed and joint initiation will occur (Fig. 10). At Cx43 levels above the threshold, *evx1* is not sufficient for joint initiation and a joint is not formed. At Cx43 levels at/below the threshold, *evx1* expression is less suppressed by Cx43, so *evx1* expression increases and can initiate joint formation. We suggest that in *sof*^{b123} mutants (which exhibit reduced *cx43* mRNA) (Iovine et al., 2005), or when Cx43 levels are otherwise reduced (Fig. 7), fin rays achieve the threshold of Cx43 activity sooner and trigger premature joint initiation. In contrast, when Cx43 levels are too high, joint initiation fails completely. If the level of Cx43 activity is only modestly higher than wild-type (as in *alf*^{dty86} mutants), then *cx43* levels are less likely to be reduced to the required threshold, causing *evx1* expression and joint formation to become stochastic (Sims et al., 2009). Note that because *miR-133a* has multiple targets (Yin et al., 2008), we cannot rule out the possibility that another targeted gene mediates the observed effects on *evx1* expression and joint formation. However, our prior findings on the role of Cx43 in suppressing joint formation (Hoptak-Solga et al., 2008; Sims et al., 2009) are consistent with the proposed model.

Cx43 is expressed in cells of two distinct lineages in the regenerating fin: in the dermal fibroblasts and in the joint-forming osteoblasts (Sims et al., 2009). Our findings reveal that Cx43 activity in the dermal fibroblasts is responsible for rescuing both regenerate length and segment length in *sof*^{b123} fins. Regenerate length is influenced by the number of proliferating cells, which Cx43 may influence autonomously (Hoptak-Solga et al., 2008). Segment length is regulated by the timing of joint formation, which we show here is determined by a transient reduction in Cx43 that permits *evx1* expression, and therefore differentiation of joint-forming osteoblasts from among the lateral skeletal precursor cells. Interestingly, joint-forming cells and bone-forming cells are both derived from a common precursor population (Tu and Johnson, 2011). Therefore, we suggest that the level of Cx43 activity in the dermal fibroblasts is responsible for influencing joint-forming cell differentiation. This mechanism ensures that joint-forming cells initiate a joint at the appropriate time and

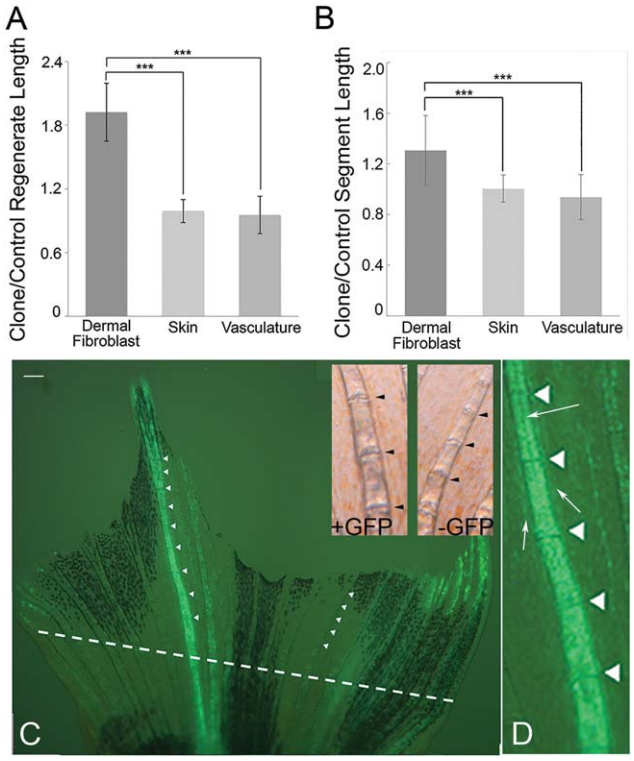

Fig. 9. Expression of Cx43 in dermal fibroblasts rescues both regenerate length and segment length. **A**: Regenerate length is significantly increased in fins where Cx43 is induced in dermal fibroblasts, but not in fins where Cx43 is induced in other lineages. **B**: Segment length is significantly increased in fins where Cx43 is induced in dermal fibroblasts, but not in fins where Cx43 is induced in other lineages. Both regenerate and segment length measurements were taken as the ratio of the GFP-positive clone length over the analogous fin ray on the opposite side of the fin. Statistically significant differences were determined by the Student's *t*-test, where $P < 0.001$ (***). Error bars represent the standard deviation. **C**: Representative image of a fin containing a GFP-positive clone in the dermal fibroblasts. The amputation plane is indicated by a dotted line. Scale bar = 150 μm. Insets show higher magnification views of a region of both the GFP-positive fin ray and in the contralateral GFP-negative fin ray (bright-field is shown to better visualize the joints). Joints are indicated as arrowheads in both the GFP-positive fin ray and in the GFP-negative fin ray. **D**: Higher magnification view of the GFP-positive clone to show GFP expression in dermal fibroblasts. Dermal fibroblast clones are notable for the ability to see the unlabeled artery running down the middle of ray (arrow pointing to middle of ray), whereas osteoblast clones obscure the artery. Dermal fibroblast clones also show distinct GFP-positive fibroblast cells that are adjacent to, but not contained within, the ray itself (arrows pointing to GFP-positive cells flanking the ray), whereas osteoblast clones remain strictly associated with the hemirays.

TABLE 2. GFP Clone Types and Rescue of *sof*^{b123} Fin Phenotypes

Clone type	Rescue	Fail
Osteoblast	1	20
Epidermis	3	16
Fibroblast	17	9
Lateral line	0	9
Vasculature	0	5
Pigment	0	1
Intraray glia	0	1
Blood	0	2

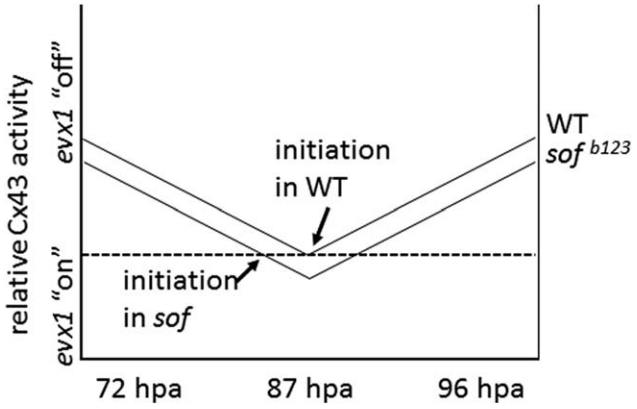

Fig. 10. Cx43 threshold model for joint initiation. Cx43 activity levels decrease to a threshold level, allowing for *evx1* expression and, therefore, joint initiation. In the *sof*^{b123} mutant, where *cx43* mRNA levels are reduced with respect to WT, the threshold is reached sooner, inducing premature joint initiation and resulting in short segments.

place, and in a manner that is coordinated with regenerate length.

Several questions remain. For example, by what mechanism(s) is Cx43 activity reduced? Our findings suggest that Cx43 activity cycles in concert with joint formation, but the identity of the factor(s) controlling these oscillations is unknown. To what extent must Cx43 activity be reduced to achieve the proposed threshold for *evx1* expression? Here, we find a modest reduction in *cx43* mRNA correlates with joint initiation. However, this does not rule out the possibility that Cx43 activity is influenced through additional mechanisms, such as an increase in turnover at the plasma membrane or inactivation of gap junction channels. Finally, by what mechanism(s) do the dermal fibroblasts communicate with the precursors of the osteoblast lineages? In a prior study, we showed that Cx43 activity is required for the expression of the growth factor, *sema3d*, in cells of the lateral osteoblast lineage (which also appears to act upstream of joint formation) (Ton and Iovine, 2012). We have proposed that these cells may communicate directly, via heterotypic gap junction channels. Alternatively, communication may be indirect, through the secretion of a growth factor by the dermal fibroblasts that is recognized by a cell surface receptor in the precursors of the osteoblast lineages (Ton and Iovine, 2013a). Studies to distinguish these possibilities are ongoing.

Future studies are aimed at revealing the mechanisms for regulating Cx43 activity during skeletal regeneration, and at revealing how changes in Cx43 activity influence changes in gene expression. Given that so little is understood regarding the appropriate positioning of joints, we anticipate that our findings will continue to provide important insights into this question.

Experimental Procedures

Fish Maintenance

Zebrafish were raised at constant temperature of 28 °C in a 14 light:10 dark photo period. C32, *sof*^{b123}, *alf*^{dty86} *Tg(hsp70:miR-133sp)*^{pd48}, and *Tg(hsp70:miR-133a1)*^{pd47} were used. The transgenic lines were generously provided by V.P. Yin. Research was performed as described to the IACUC for Lehigh University

(protocol #187, 3/14/2016 approval). For induction of transgene expression, fish were placed in a tank of fish water heated to 37 °C for 1 hr, followed by a gradual cooling back to 28 °C.

In Situ Hybridization

Antisense digoxigenin-labeled probes were generated as described (Iovine et al., 2005 for *cx43*; Ton and Iovine, 2013b for *evx1*). Whole-mount ISH was completed as described (Sims et al., 2009). To evaluate the relative level of gene expression, whole-mount ISH was completed on four fins in each of three independent experiments (12 fins per group). For ISH on cryosections, fins were fixed following the same fixation conditions, methanol dehydration, and gradual rehydration as in whole-mount ISH; harvested fins were then embedded in 1.5% agarose/5% sucrose and equilibrated overnight in 30% sucrose. Those blocks were mounted in OCT and cryosectioned using the Reichert-Jung 2800 Frigocut cryostat. 15-μM sections were mounted on Superfrost Plus slides (Fisher) and air-dried overnight at room temperature. ISH on cryosections was completed as described (Ton and Iovine, 2013b). To evaluate the relative level of gene expression, cryo-ISH was evaluated from five sections from each of three different fins.

Joint Morphology Time Course

To establish the time course for joint initiation, fins were amputated at the 30% level (just proximal to the cleft) and allowed to regenerate for 2–5 days. Fins were harvested and processed for ZNS5 immunofluorescence (below) and examined using the 40x N.A. 1.4 PlanApo objective on a Zeiss LSM 510 META confocal microscope to identify joint cell morphology as described (Sims et al., 2009).

ZNS5 Immunofluorescence

Fins were harvested and fixed overnight in 4% paraformaldehyde/PBS at 4 °C then stored in methanol at -20 °C. Fins were rehydrated in successive washes in decreasing methanol/PBS solutions. After block (2% BSA/PBS), fins were treated with 1:200 ZNS5 (ZIRC) in block at 4 °C overnight. Following three washes in block, fins were treated with secondary antibody (Alexa 488 or Alexa 546) at 1:200 overnight at 4 °C and washed in block again before mounting on slides. Fins were mounted on Superfrost slides in glycerol. Fins were examined on a Zeiss confocal microscopy to evaluate joint morphology and using a Nikon Eclipse E80 microscope with a Nikon digital camera to measure segment length.

qRT-PCR Analysis

Fins were amputated at the 30% level and allowed to regenerate for 72, 87, or 96 hpa. Total RNA was isolated from 5–10 harvested fins using TRIzol reagent (Gibco), and cDNA was synthesized using oligo-dT and reverse transcriptase. Diluted cDNA (1:100 for *cx43* and 1:10 for *evx1*) was combined with Qiagen Sybr Green PCR master mix and with either *cx43* or *actin* (control) primers. Samples were run using the Rotor Gene Real Time PCR system, and average cycle number (C_T) was determined for each amplicon. ΔC_T represents the normalized gene level with respect to the *actin* control. Three biological replicates of each sample were prepared. Within each biological replicate, two technical replicates for *cx43* and *actin* reactions were completed. The average values for the technical replicates are shown for each biological replicate (Table 1).

FK506 Treatment

For evaluation of segment length and regenerate length, fins were amputated at the 50% level (these measurements are taken at 5 dpa and do not rely on the timing of the formation of the first joint). Fish were treated for 3 consecutive days starting 48 hpa with 0.1 μg/mL FK506 (fresh each day). At 5 dpa fish were treated for either ZNS5 staining (fixed tissue) or calcein staining (live tissue, see below). The third fin rays of both the dorsal and ventral sides (V+3, D+3) were examined for regenerate and segment length measurements, as established (Iovine and Johnson, 2000). Regenerate length was measured from the amputation plane to the distal end of the fin, and segment length was measured as the distance between the two proximal-most joints. Student's *t*-tests were performed to determine if data sets were statistically different ($P < 0.05$).

For evaluation of gene expression at the time of joint initiation, fins were amputated at the 30% level, treated with 0.1 μg/mL FK506 (n = 5) or DMSO (n = 5) at 72 hpa for 15 hr, and harvested at 87 hpa. These fins were processed for ISH to detect *evx1* expression.

Calcein Staining

Calcein staining was performed to detect calcified bone matrix (Du et al., 2001). A 0.2% calcein solution was prepared by dissolving 2 g calcein powder (Sigma) in 1 L deionized water; 0.5M NaOH was added to bring the pH to neutral. Zebrafish were immersed in the solution for 15 min, followed by several rinses with clean water and 10 min in fresh water to allow unbound calcein to diffuse out of the tissue. Zebrafish were then anesthetized in tricaine, viewed at 4X using a Nikon Eclipse 80i microscope with green fluorescence filters, and imaged using a Nikon digital camera.

Chimeric Analysis

The *cx43* open reading frame was amplified from a 96-hr-postfertilization (hpf) cDNA library using primers cx43-F 5' GGCGGCGATCGCTTAATTAAATGGGTGACTGGAGTGC and cx 43-R 5' TCGACCTGCAGGTTAATTAAGACGTCCAGGTCATCAGG. The PCR product was cloned via Gibson assembly into the hsp-PT2 transposon plasmid, downstream of the *hsp70l* promoter using the Pac I site. The resulting molecule contains two functional cassettes: a ubiquitously expressed GFP driven by the Xenopus EF1a promoter for identifying cells that have integrated the transposon, and the *hsp70l* promoter driving *cx43* for overex pressing the wild-type protein when fish are exposed to heat shock.

soj^{b123} embryos were injected at the 1-cell stage with a mixture of *hsp:cx43*-pT2 plasmid DNA at 50 ng/uL and transposase mRNA at 15 ng/uL (as described in Tryon and Johnson, 2012). All GFP-positive fish were grown to adulthood (5–6 months) and screened for caudal fin clones. GFP-positive clones were assigned to the appropriate lineage class based on the cellular and clone morphologies as described previously (Tu and Johnson, 2011). Caudal fin clones were subsequently amputated across the GFP-positive clone such that the labeled cells would contribute to the blastema and, ultimately, the regenerated fin tissue. Fish were

grown for 4 weeks while being exposed to a daily heat pulse of 38 °C for 30 min and were imaged weekly to identify atypical growth during regeneration. The Nikon SMZ 1500 microscope with 1.6X WD 24 Nikon HR Plan Apo objective was used to visualize clones, and images were collected using a Jenoptik L.O.S. GmbH camera and ProgResC14 software.

Adobe Illustrator was used to measure the relative lengths of segments and rays in fins. A line (or series of lines, in the case of a curved regenerated ray) was superimposed over the photographed image for both the GFP-positive labeled ray and its contralateral counterpart. The measure tool in Adobe Illustrator was subsequently used to determine the length of each feature in points.

Acknowledgments

The authors wish to thank Rebecca Bowman for care of the animal facilities, and Voot Yin for the *miR133a* transgenic lines. The authors also thank members of the Iovine and Johnson labs for thoughtful comments on the article. We thank the Zebrafish International Research Center for providing the monoclonal ZNS5 antibody for reasonable cost. This work was supported in part through funding to M.K.I. (NIH grant number R15HD080507) and S.L.J. (NIH grant number R01GM056988).

References

Banerji R, Eble DM, Iovine MK, Skibbens RV. 2016. Esco2 regulates cx43 expression during skeletal regeneration in the zebrafish fin. Dev Dyn 245:7–21.

Borday V, Thaeron C, Avaron F, Brulfert A, Casane D, Laurenti P, Geraudie J. 2001. evx1 transcription in bony fin rays segment boundaries leads to a reiterated pattern during zebrafish fin development and regeneration. Dev Dyn 220:91–98.

Brown AM, Fisher S, Iovine MK. 2009. Osteoblast maturation occurs in overlapping proximal-distal compartments during fin regeneration in zebrafish. Dev Dyn 238:2922–2928.

Du SJ, Frenkel V, Kindschi G, Zohar Y. 2001. Visualizing normal and defective bone development in zebrafish embryos using the fluorescent chromophore calcein. Dev Biol 238:239–246.

Hoptak-Solga AD, Nielsen S, Jain I, Thummel R, Hyde DR, Iovine MK. 2008. Connexin43 (GJA1) is required in the population of dividing cells during fin regeneration. Dev Biol 317:541–548.

Iovine MK, Higgins EP, Hindes A, Coblitz B, Johnson SL. 2005. Mutations in connexin43 (GJA1) perturb bone growth in zebrafish fins. Dev Biol 278:208–219.

Iovine MK, Johnson SL. 2000. Genetic analysis of isometric growth control mechanisms in the zebrafish caudal Fin. Genetics 155: 1321–1329.

Knopf F, Hammond C, Chekuru A, Kurth T, Hans S, Weber CW, Mahatma G, Fisher S, Brand M, Schulte-Merker S, Weidinger G. 2011. Bone regenerates via dedifferentiation of osteoblasts in the zebrafish fin. Dev Cell 20:713–724.

Kujawski S, Lin W, Kitte F, Bormel M, Fuchs S, Arulmozhivarman G, Vogt S, Theil D, Zhang Y, Antos CL. 2014. Calcineurin regulates coordinated outgrowth of zebrafish regenerating fins. Dev Cell 28:573–587.

Lee Y, Grill S, Sanchez A, Murphy-Ryan M, Poss KD. 2005. Fgf signaling instructs position-dependent growth rate during zebrafish fin regeneration. Development 132:5173–5183.

Pacifici M, Koyama E, Shibukawa Y, Wu C, Tamamura Y, Enomoto-Iwamoto M, Iwamoto M. 2006. Cellular and molecular mechanisms of synovial joint and articular cartilage formation. Ann NY Acad Sci 1068:74–86.

Perathoner S, Daane JM, Henrion U, Seebohm G, Higdon CW, Johnson SL, Nusslein-Volhard C, Harris MP. 2014. Bioelectric signaling regulates size in zebrafish fins. PLoS Genet 10: e1004080.

Schulte CJ, Allen C, England SJ, Juarez-Morales JL, Lewis KE. 2011. Evx1 is required for joint formation in zebrafish fin dermoskeleton. Dev Dyn 240:1240–1248.

Sims K Jr, Eble DM, Iovine MK. 2009. Connexin43 regulates joint location in zebrafish fins. Dev Biol 327:410–418.

Ton QV, Iovine MK. 2012. Semaphorin3d mediates Cx43-dependent phenotypes during fin regeneration. Dev Biol 366: 195–203.

Ton QV, Iovine MK. 2013a. Determining how defects in connexin43 cause skeletal disease. Genesis 51:75–82.

Ton QV, Iovine MK. 2013b. Identification of an evx1-dependent joint-formation pathway during FIN regeneration. PloS One 8: e81240.

Tryon RC, Johnson SL. 2012. Clonal and lineage analysis of melanocyte stem cells and their progeny in the zebrafish. Methods Mol Biol 916:181–195.

Tryon RC, Johnson SL. 2014. Clonal analysis of kit ligand a functional expression reveals lineage-specific competence to promote melanocyte rescue in the mutant regenerating caudal fin. PloS One 9:e102317.

Tu S, Johnson SL. 2011. Fate restriction in the growing and regenerating zebrafish fin. Dev Cell 20:725–732.

van Eeden FJ, Granato M, Schach U, Brand M, Furutani-Seiki M, Haffter P, Hammerschmidt M, Heisenberg CP, Jiang YJ, Kane DA, Kelsh RN, Mullins MC, Odenthal J, Warga RM, Nusslein-Volhard C. 1996. Genetic analysis of fin formation in the zebrafish, Danio rerio. Development 123:255–262.

Yin VP, Lepilina A, Smith A, Poss KD. 2012. Regulation of zebrafish heart regeneration by miR-133. Dev Biol 365:319–327.

Yin VP, Thomson JM, Thummel R, Hyde DR, Hammond SM, Poss KD. 2008. Fgf-dependent depletion of microRNA-133 promotes appendage regeneration in zebrafish. Genes Dev 22: 728–733.